Low-cost Refrigerator Frost Detection using Piezoelectric Sensors

Zhijian Yang, Siddharth Rupavatharam, Alexis Burns, Daewon Lee, Richard Howard, Volkan Isler
Samsung Artificial Intelligence Center New York

***Abstract*—Frost accumulation on refrigerator evaporator coils is a significant source of wasted energy. While automatic defrosting is a standard feature on modern refrigerators, current commercial solutions use heuristics to determine the frequency of heating cycles, leading to a sub-optimal defrosting routine. The majority of previous defrosting research incorporates cameras or microwave technology to better inform defrost algorithms of frost accumulation, however, these methods are both financially and computationally expensive. In this paper, we propose a low-cost frost detection system using ultrasonic resonance of piezoelectric sensors. We addressed the financial and computational cost challenges by using low-cost sensors and basic circuit components to replace software complexity. Our frost detection system was evaluated extensively in a Samsung refrigerator, resulting in a frost detection accuracy of 99.7%. We believe our solution can be further used for downstream refrigerator control cycle optimizations to achieve improved energy efficiency.**

***Index Terms*—piezoelectric, resonance, sensing, frost detection**

I. Introduction

Refrigerators are essential home appliances that run 24 hours a day, 365 days a year. Although advances in materials and methods of insulation have greatly increased cooling efficiency of refrigerators [1], they still constitute about 7% of the total energy consumed at home [2], with their active cooling systems using a significant portion of that energy. Frost that forms on the heat exchange evaporator coils is undesirable as it reduces cooling efficiency, increasing energy consumption [3]. Therefore, reliably detecting the accumulated frost is necessary to eliminate it an in informed manner. Figure 1 shows the evaporator coil with and without frost.

To maintain the refrigerator at a cold temperature, the warm air inside is circulated over the surface of an evaporator coil that has cold coolant flowing through it. The heat from the air is transferred to the cold evaporator coil reducing the temperature of the air. The coolant flowing inside the evaporator carries away the heat to the exterior of the refrigerator. However, moisture present in the warm air condenses on the evaporator coil and freezes forming frost. This layer of frost contains trapped air, that acts as a layer of insulation over the evaporator coil making heat exchange inefficient. A small layer of insulating frost over the primary heat exchange surface significantly impacts energy efficiency.

While automatic defrosting is a standard feature in modern refrigerators, current methods rely on heuristics such as internal temperature and refrigerator door opening frequency to estimate the amount of frost accumulation [4]. Unreliable frost detection mechanisms lead to untimely defrosting cycles; too frequent heating cycles deteriorate food, while too infrequent cycles lead to frost accumulation affecting cooling efficiency.

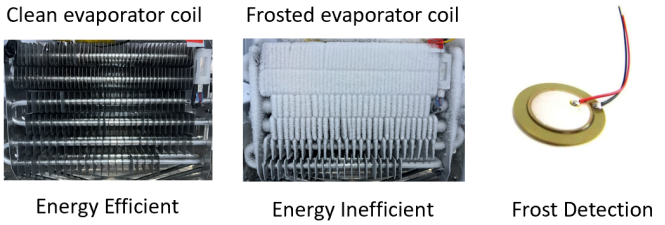

Fig. 1. Frost accumulated on a refrigerator evaporator coil insulates it, impeding heat transfer and reducing cooling efficiency. We propose a low-cost frost detection sensing system that leverages changes in resonance frequency of a piezoelectric sensor.

Multiple solutions leveraging cameras [5], microwave resonators [6], and capacitance-based methods [7] have been proposed to detect accumulation of frost on various surfaces. However, these solutions require high cost sensors and do not translate well to refrigerators. Camera based solutions are susceptible to frost formation on the lens, line-of-sight blockage, and are reliant on proper lighting inside the refrigerator. Microwave resonators use specialized hardware that are expensive to engineer and miniaturize. On the other hand, acoustic based solutions which can be low-cost, miniaturizable, and independent of environmental factors are sparsely explored.

In this paper, we focus on utilizing ultrasonic piezoelectric [8] sensors (as shown in Figure 1(c)) for frost detection. Our key insight is that being low-cost and light-weight, any small amount of mass attached to the piezoelectric sensor will change its physical property, thus revealing information of frost formed on the sensor. Specifically, we ask the following research question: *Can changes in resonance frequency of a piezoelectric crystal be used to detect accumulation of frost?* Piezoelectric crystals generate an electric charge when compressed, and vibrate when an electric charge is applied [8]. The nature vibration frequency of a piezoelectric sensor is called resonance frequency. Mass deposition on the crystal changes both the resonance frequency and the amplitude of vibrations, which can be measured through custom designed circuits. While similar principles have been applied in monitoring thin film deposition for electronics manufacturing [9], transferring the idea to frost detection brings its own unique challenges.

Resonance properties of piezoelectric crystals are temperature dependent, in additional to being affected by mass deposition onto the sensor. The temperature near the evaporator coil varies from $-30°C$ to $0°C$ between cooling cycles. This makes delineating frequency and amplitude changes due to frost mass accumulation from temperature changes challenging. Next, accumulating frost on the piezoelectric crystal is non-trivial. Frost forms on the coldest part of the refrigerator (i.e., evaporator coil). However, to measure the

self-resonating frequency, we cannot attach the sensor directly to the evaporator coil, as physical coupling will significant affect resonance property.

We overcome these challenges by designing a custom mount to hold the piezoelectric crystal while being thermally connected to the evaporator coil, this enables accumulating frost reliably. We also develop a software online-calibration scheme to compensate temperature variations.

To the best of our knowledge, we built the first system that leverages low cost piezoelectric sensor for frost detection inside refrigerators, specifically our contributions are as follows:

1. **Frost detection circuit:** We designed a custom circuit for frost detection using low-cost components based on piezoelectric sensor resonance property
2. **Isothermal sensor mount:** We built a mount to both physically support the piezoelectric crystal and maintain the same temperature as the coil
3. **Temperature calibration:** We developed a software calibration pipeline to detect frost over the wide operating temperature of the refrigerator
4. **Real world evaluation:** We demonstrated the performance of our system in a real working environment. Our system shows over 99% accuracy in detecting frost when tested over multiple days in a Samsung refrigerator

Our solution consists of low-cost hardware; a 20-cent piezoelectric crystal, commercial off the shelf available active and passive electronic components. It is small in size, inaudible to humans and their pets, and can be run with the computation power of a microcontroller. We believe our sensing system can be used as a reliable source of frost data to optimize the timing of refrigerator defrost cycles leading to energy savings.

The paper is organized as follows, we first discuss the physics behind resonance frequency changes, then describe our system design in detail, followed by evaluation and results.

II. Physics Basics

This section presents relevant background for this paper, centered around resonance frequency, effects of mass loading and temperature on the piezoelectric crystal.

A. Resonance frequency

Objects vibrate at a natural frequency dependent on their physical structure known as resonance frequency. They vibrate at the highest amplitude possible when external energy is applied at their resonance frequency [10]. In this paper, we detect the presence of frost by monitoring changes in the resonance frequency of a piezoelectric crystal, with it being modeled as a spring-mass system whose resonance frequency changes with, (1) an attached mass and (2) temperature.

B. Mass attached to sensor

Figure 2(a) shows the change in resonance frequency when a drop of water was placed on a vibrating piezoelectric sensor. When the mass on the piezoelectric crystal was increased, the amplitude of vibrations and resonance frequency was observed to decrease. The frequency and amplitude characteristics of the piezoelectric crystal were measured using a vector network analyzer [11]. The impedance of the sensor was measured to lie in the range of 200 to 700 Ω. We observed a dip in the impedance curve at around 45 kHz when the crystal freely vibrated in air, which then shifted to 42 kHz as the drop of water was placed, signifying a decrease in resonance frequency. Hence, we expect to observe a similar shift in frequency when frost accumulation mass loads the piezoelectric crystal.

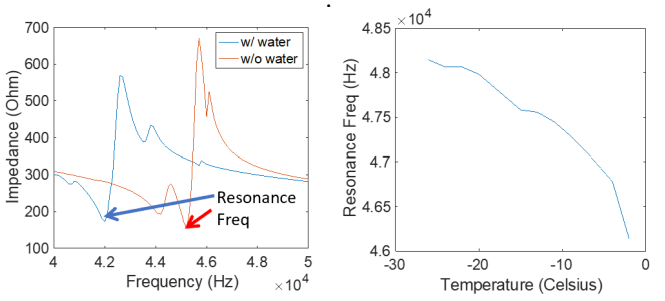

(a) (b)

Fig. 2. (a) Electrical impedance of a piezoelectric sensor is minimum at the resonance frequency. A drop of water placed on the piezoelectric sensor increases the mass of the sensor, decreasing the resonance frequency from around $45kHz$ (red) to $42kHz$ (blue). (b) Temperature's effect on resonance frequency: resonance frequency decreases with increasing temperature.

C. Temperature's effect

The internal temperature of the refrigerator near the evaporator coil varies drastically over time. The temperature in the region can drop to as low as -30 degrees Celsius during a cooling cycle, and rise to as high as 0 degrees Celsius during a defrosting cycle. This dramatic temperature change affects the internal structure of the piezoelectric sensor affecting its resonance frequency [12]. Figure 2(b) shows the resonance frequency of the piezoelectric sensor across different temperatures. It is possible that temperature effects have greater contribution to changes in resonance frequency than mass loading due to frost. Thus, to properly understand and detect frost accumulation, we needed to compensate and account for the temperature at which the amplitude is measured.

In this paper, we accurately detected frost accumulation on a piezoelectric sensor, while compensating for the changing stiffness of the sensor over the evaporator coil's operating temperature of -30 to 0 degrees Celsius. Additionally, we performed sensing in the ultrasonic range, above 100 kHz, to remain inaudible to humans and animals in homes.

III. System Design

Our system consists of a sinusoidal signal generator circuit, a piezoelectric sensor with signal mixing circuit, and a software calibration and frost detection routine as shown in Figure 3. The piezoelectric sensor is designed and mounted to ensure frost accumulation on the sensor occurs at a similar rate to the evaporator coil. The signal generator circuit generates an AC voltage to excite the piezoelectric sensor. The signal mixing circuit demodulates received signal to obtain information corresponding to frost formation which is fed to a detection

algorithm. The software calibration pipeline ensures robust system performance over long periods of time. We realize our system using low-cost off-the-shelf circuit components and computationally efficient algorithms.

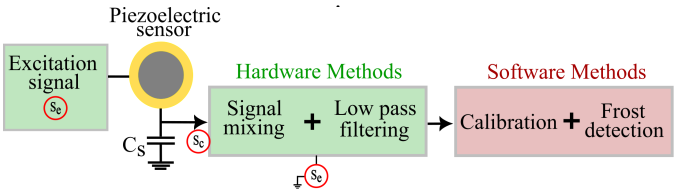

Fig. 3. System architecture: our sensing system is comprised of (i) a signal generator that produces $24V_{pp}$ AC signals up to 150 kHz, (ii) a piezoelectric sensor in series with a capacitor that are excited using AC signals, (iii) a signal mixing and low pass filtering circuit that extracts signal changes corresponding to frost accumulation from the transmitted signal, and (iv) a microcontroller for digitizing the sensed signal, perform calibration and run software routines for frost detection

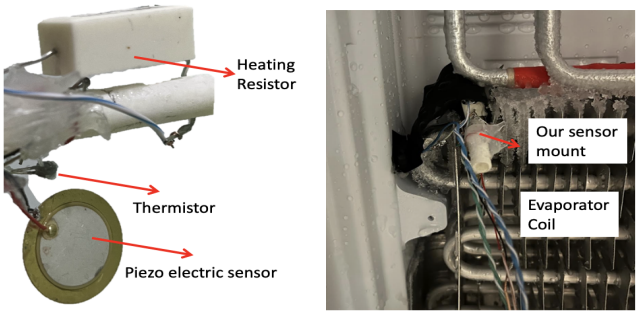

(a) (b)

Fig. 4. Sensor deployment: (a) our sensor front end hardware consists of a piezoelectric sensor, a thermistor, and a heating resistor. (b) We deploy our sensor between the blades of the evaporator coil, so that the sensor system will have almost the same temperature as the evaporator coil and frost will grow on the piezoelectric sensor.

A. Sensor design and deployment

As described in Section. II, changes in resonance frequency of a piezoelectric sensor due to mass loading are leveraged to sense frost formation. To perform effective resonance shift sensing: (i) frost needs to accumulate on the sensor, and (ii) the piezoelectric sensor should only physically make contact with frost.

For (i), we observe that frost starts accumulating on the coldest part in the refrigerator (i.e., the evaporator coil) [13] and mount the sensor as close to the evaporator coil as possible (between the blades of the evaporator coil) while ensuring no contact occurs between the sensor and the coil. We then connect the exterior of the signal wires (i.e., Ground and S_e) attached to the piezoelectric sensor to the evaporator coil using aluminum tape to thermally connect them. The sensor now follows the temperature of the evaporator coil as heat from the sensor is transferred over the wires. This mounting arrangement ensures frost accumulates on the sensor at a similar rate as the evaporator coil.

For (ii), we make sure that the sensor does not touch any surrounding components. This is achieved by hanging the sensor using the signal wires attached to it as shown in Figure 4. Piezoelectric crystals are extremely sensitive to contact including delicate touches, which significantly changes their resonance frequency. Physical contact with surroundings changes the baseline resonance frequency as the sensor mass is now coupled to the surrounding mass at the contact point. Therefore, the sensor is positioned such that it only makes contact with frost that accumulates on it.

To monitor and compensate for temperature related effects on resonance, we place a thermistor close to the piezoelectric sensor. A heating resistor for removing residual frost for baseline calibration is also included in the sensor mount (will be elaborated in section III-C).

B. Signal processing

As shown in Figure 3, we connect the piezoelectric sensor in series with a capacitor C_s, and drive the circuit with the excitation signal S_e with fixed frequency f_0. (f_0 also equals to the resonance frequency of the clean sensor without frost). The piezoelectric sensor acts like a band pass filter, with center frequency being resonance frequency f_0. When frost forms, the resonance frequency will decrease, leading to shift of the band-pass curve and thus excitation signal S_e deviating from the resonance frequency. This eventually leads to decrease in the signal amplitude across the capacitor S_c. We using signal mixing techniques to extract this change in amplitude, and perform frost detection. We will elaborate on how we realize this idea using basic circuit components.

1) Excitation signal (S_e): A printed circuit board connected with a refrigerator micro-controller output pin was designed to create AC signals to excite the piezoelectric sensor. The circuit schematic is shown in Figure 6.

A pulse width modulated signal (A_{pwm}) from a microcontroller is used to toggle the gate of a MOSFET on and off, with the drain connected to a fixed DC voltage (V_{dd}). The output square wave is filtered using a two-stage low pass filter to smooth out the signal and produce a sine wave. This sine wave is then input to the gate of a DC-biased MOSFET amplifier. A capacitor is connected to the drain to remove the DC-bias. The filtered sine signal is then input to the inverting terminal of an operational amplifier, which is used to provide additional gain from a low output impedance source. Component values of the circuit are: R1: 100 Ω, R2: 10 kΩ, R3, R8: 1 kΩ, R4, R5, R6: 5.6 kΩ, R7: 10 kΩ tunable potentiometer, R9, R10: 10 kΩ, C1, C2: 300 pF, M1, M2: IRLZ34N, OA1: TLE2081.

2) Signal mixing: The signal amplitude S_c across the capacitor will change according to the amount of frost on the sensor. To extract this amplitude change, we use signal mixing. A copy of the excitation signal $S_e = Asin(2\pi ft + \phi_1)$ is multiplied with the signal obtained from across the capacitor, $S_c = Bsin(2\pi ft + \phi_2)$ using an analog mixer chip [14]–[16].

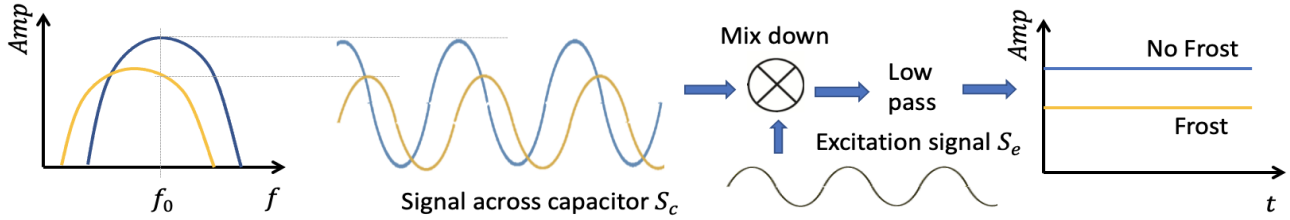

Fig. 5. Signal mixing visualization: (a) Resonance frequency curves of a piezoelectric sensor with (yellow) and without frost (blue). Accumulated frost acts as a mass reducing amplitude of vibrations and shifting the resonance frequency left, (b) which leads to signal amplitude across the capacitor S_c to decrease. The AC signal S_c is mixed with the original excitation signal S_e and low pass filtered to obtain the amplitude of S_c. (c) Frost is detected by comparing the obtained DC amplitude with a calibrated baseline amplitude for a given temperature.

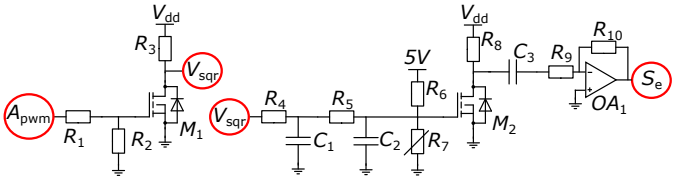

Fig. 6. Excitation signal circuit: a PWM signal from the microcontroller is used to toggle a MOSFET gate to generate a high voltage square wave. The square wave then passes through two stage R-C low pass filter to form a sinusoidal signal that is further amplified and applied as excitation signal S_e.

The amplitude of the signal is given by:

$$Y(t) = \frac{AB}{2}\cos(\phi_1 - \phi_2) - \underbrace{\frac{AB}{2}\cos(2\pi(2f)t + (\phi_1 + \phi_2))}_{\text{filtered out}}, \quad (1)$$

where, A and B are the signal across capacitor and excitation signal amplitudes with corresponding phases ϕ_1 and ϕ_2. Since both signals share the same frequency, the first term is proportional to the amplitude, while the second term occurs at the sum of the frequencies. The second term is removed using a 1 Hz low pass filter. Thus, the final output after mixing and low pass filtering is:

$$\overline{Y(t)} = \frac{AB}{2}\cos(\phi_1 - \phi_2) \quad (2)$$

The signal visualization during the mixing process is shown in Figure 5.

3) Frequency selection: Piezoelectric sensors may have multiple resonance frequencies due to the mode of vibration, for example by performing a frequency sweep using a vector network analyzer, we observed that the sensor we are using has resonance frequencies at 6.8 kHz, 44 kHz, 88kHz, and 137 kHz. We chose to use a frequency close to 137 kHz to remain inaudible to humans and animals.

To accurately identify a frequency close to 137 kHz with high sensitivity to frost accumulation, we deployed the sensor in the refrigerator freezer and cooled it down to the normal working temperature of the freezer. We then excited the sensor with a frequency around 137 kHz while measuring the amplitude S_c and tuned the input signal frequency to simulate change in resonance frequency. We identified the frequency where a small change in frequency resulted in a large change in amplitude $\overline{Y(t)}$. We used this frequency to excite the sensor.

C. Software Design

A key part of the system is to obtain the mixed and low pass filtered output $\overline{Y(t)}$ at every temperature T when there is no frost and use this as a baseline. Note that the frequency response of the piezoelectric sensor is sensitive to the orientation or location of the sensor, because location and orientation affect the tension on the wire, and thus the resonance property [17]. The system needs to be re-calibrated after a certain time interval as the sensor position may slowly move over frosting and de-frosting cycles and unavoidable ambient vibrations of the refrigerator. We designed a self-calibration procedure to automate this.

When the defrost cycle starts and the refrigerator door is closed, the temperature of the evaporator coil rises to above zero degrees Celsius to melt the frost. During the period when the evaporator is cooling down to the normal working temperature, there is no frost on the evaporator coil. We use this cool-down period as an opportunity for calibration. Because frost only forms on the coldest parts of the system, we use our own heating capacitor attached to our piezoelectric sensor to slightly raise the temperature of the piezoelectric sensor above the surrounding temperature, preventing frost from growing on our sensor during the cool-down process. By doing so, we can get a clean calibrated reading without frost, for every temperature T. Using this information, we created a look up table, where each entry is a temperature and a mixer output pair ($< T, \overline{Y(t)} >$) when there is no frost. We make our frost / no frost decision based on comparing measured mixer output value $\overline{Y(t)}$ with the baseline value from the lookup table at the same temperature T.

IV. Evaluation

In this section, we first discuss experiments and results for frost detection using our system when deployed in a Samsung refrigerator under real-world settings. A system level evaluation of the total cost will then follow, to prove the feasibility for real world deployment.

A. Frost detection results

Experiments We deployed our sensor in a Samsung refrigerator and removed the internal back panel to expose the

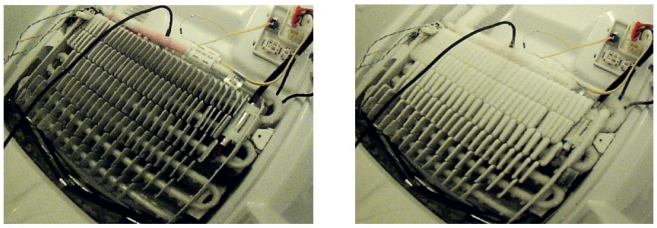

(a) Without frost (b) With frost

Fig. 7. Close-up images of the evaporator coil obtained using the ground truth camera. The looping cylindrical tubes circulate low temperature coolant with metal fins providing a large surface area for heat transfer.

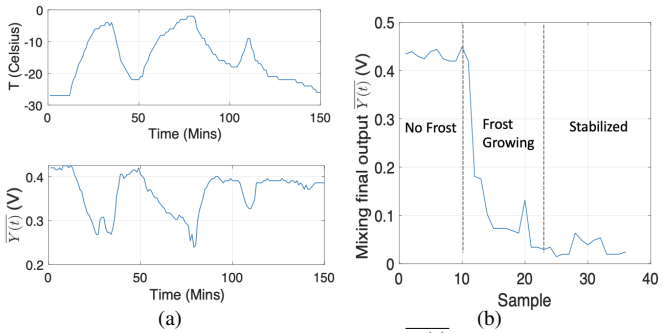

(a) (b)

Fig. 8. (a) When no frost exists, mixed output $\overline{Y(t)}$'s change correlates well with temperature change T. (b) When temperature is constant, mixed output $\overline{Y(t)}$ decreases with increasing amount of frost.

evaporator coil to the ground truth camera. Frost grew due to door opening and closing to let the moisture in the air enter the freezer and condense on the evaporator coil. We collected experimental data across multiple different days, and provided evaluation results for our system.

Ground truth definition The ground truth was obtained by deploying a camera inside the refrigerator. When the evaporator looked mostly white from the camera view, we defined it as has frost (Figure 7(a)). When the evaporator was mostly free of frost, we defined it as no frost (Figure 7(b)). Each measurement was labeled manually as frost or no frost based on visual information. For the small, initial amounts of frost during the accumulation period, due to the difficulty in defining ground truth frost levels, we did not perform frost detection on those frames.

Frost detection results Figure 8(a) visualizes the change of temperature T and mixed output reading $\overline{Y(t)}$ over time during our experiments, when there was no frost. Observe that the trends of T and $\overline{Y(t)}$ are closely correlated: $\overline{Y(t)}$ increases with the decrease of T. This aligns well with the explanation in section II. Figure 8(b) shows the change of the mixed output $\overline{Y(t)}$ over time, while the temperature is kept constant (at $-17°C$) and frost is accumulating. It is evident that the frost formulation phase decreases the value of $\overline{Y(t)}$, proving the explanation in Figure 5.

Figure 9 aggregates and visualizes the data points collected on one of the experimental days, in the format of temperature and mixed output pair $< T, \overline{Y(t)} >$. We use a microcontroller ADC to sample the final circuit output $\overline{Y(t)}$. We observed a

TABLE I
FINAL FROST DETECTION RESULTS. WE ACHIEVE ON AVERAGE 99.7% ACCURACY FOR FROST AND NO FROST DETECTION.

GT \Est.	Frost	No Frost
Frost	99.6 %	0.4 %
No Frost	0.3 %	99.7 %

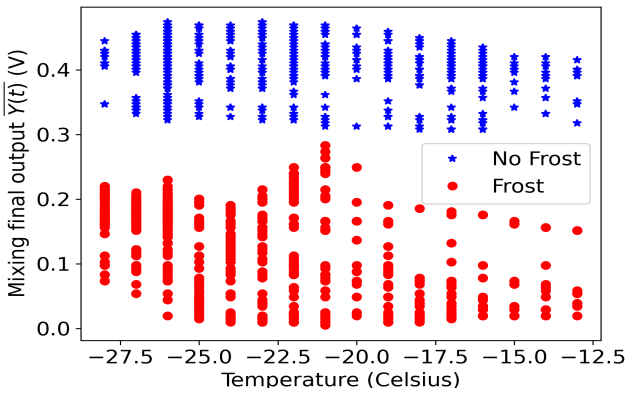

Fig. 9. Mixing final output $\overline{Y(t)}$ across different temperature T. We observe a clear separation between frost and no frost samples.

clear separation between frost and no frost data points. We trained our threshold based on the clean, no frost baseline data collected during the calibration process, and tested it on data collected for the rest of the day. This process was repeated across multiple days, and the final results are shown in the table I. Overall, 2000 samples containing frost / no frost measurements were collected, with both scenarios roughly equally distributed. On average, we achieve 99.7% frost and no frost detection accuracy for our system.

B. Cost of the sensing system

A detailed break down of the entire sensing system cost is in Table II and includes all the circuit components and sensors. All price values are calculated assuming an order size of 5000 units, except the mixer IC at 1000 units. The entire sensing system costs $11.7, with the mixing chip contributing around 80%. We believe with mass production, the cost will be further reduced and well below the budget limit for such critical sensing systems. We did not include the cost of the micro-controller here because it will always be a component of a smart refrigerator. We reuse it without adding extra cost.

V. RELATED WORK

While optimizing the refrigeration system design to reduce frost decreases the need for defrost cycles, there remained a need to properly detect when frost *did* occur in order to begin defrosting [21]However, measuring the amount of frost is a non-trivial task. Several research studies approached frost detection using vision-based methods. Many agricultural studies rely on RGB images [22] or infrared images [23] to detect frost on crops [5]. Using image-based techniques limits frost detection to specific objects and their environments that

TABLE II
BILL OF MATERIALS: TOTAL COST OF THE ENTIRE SENSING SYSTEM (INCLUDING SENSOR AND SENSING CIRCUIT) ADDS UP TO $11.7. WITH MASSIVE PRODUCTION, THE COST WILL BE FURTHER REDUCED.

Component	Price per unit ($)	Units
Piezoelectric crystal [18]	0.20	1
Resistors (0805, Thinfilm)	0.06	10
Capacitor (0805, C0G)	0.04	3
Op-amp (TLE2081)	1.18	1
Transistors (IRLZ34N)	0.53	2
Mixer IC (AD633)	8.5	1
Heating resistor [19]	0.14	1
Thermistor [20]	0.43	1

are represented in the training dataset, leaving a need for agnostic frost detection capabilities. In addition, a complex solution is required to maintain the proper image illumination and prevent frost from developing on the lens of a camera in small, dark, and cold spaces.

In lieu of a camera, a few studies implemented other sensors for frost detection. Tai *et. al* [24] used a tapered fiber sensor to detect frost by measuring the change in the light emitted from the sensor due to frost accumulation. Cho *et. al* [7] attached a capacitive sensor to a fuel pipe and correlated the rapid decrease in capacitance with frost formation. Wiltshire *et. al* [6] utilized a planar microwave resonator to detect the formation of frost based on the change in resonant frequency, resonant amplitude, and a temperature-based quality metric [25], [26]. However, the components necessary for planar microwave resonators are costly.

The solution presented in this work differs from the related work in that it is low-cost and low-power by replacing cameras and microwave resonators with ultrasound oscillators, which are much cheaper and do not require expensive circuit components. Further ultrasonic sensing systems are compact, allowing easy integration with microcontrollers for IoT applications. This solution is also application agnostic as the piezoelectric sensor can be placed in any system to measure frost.

VI. CONCLUSION AND FUTURE DIRECTIONS

In this paper we presented a frost detection system leveraging piezoelectric sensor resonance property. By implementing the full system from basic circuit components, we achieved low-cost yet accurate detection. Our next steps for future work include estimating the amount of frost and integrating our system with defrost control, along with an end-to-end energy optimization policy based on frost level estimation.

VII. ACKNOWLEDGEMENTS

We thank Dr. Larry Jackel for insights, discussions, and comments on the manuscript. We are also grateful for other relevant Samsung teams for collaboration and support.

REFERENCES

[1] W. J. Yoon, K. Seo, and Y. Kim, "Development of an optimization strategy for insulation thickness of a domestic refrigerator-freezer," *International Journal of Refrigeration*, vol. 36, no. 3, 2013.

[2] J. Geppert and R. Stamminger, "Analysis of effecting factors on domestic refrigerators' energy consumption in use," *Energy Conversion and Management*, vol. 76, pp. 794–800, 2013.

[3] A. Biglia, A. J. Gemmell, H. J. Foster, and J. A. Evans, "Temperature and energy performance of domestic cold appliances in households in england," *International Journal of Refrigeration*, vol. 87, 2018.

[4] M. F. Vitor, A. dos Santos Silveira, and R. C. C. Flesch, "Ambient virtual sensor based defrost control for single compartment refrigerators," *Applied Thermal Engineering*, vol. 166, p. 114652, 2020.

[5] Z. Li, W. Wang, Y. Sun, S. Wang, S. Deng, and Y. Lin, "Applying image recognition to frost built-up detection in air source heat pumps," *Energy*, vol. 233, p. 121004, 2021. [Online]. Available: https://www.sciencedirect.com/science/article/pii/S0360544221012524

[6] B. Wiltshire, K. Mirshahidi, K. Golovin, and M. H. Zarifi, "Robust and sensitive frost and ice detection via planar microwave resonator sensor," *Sensors and Actuators B: Chemical*, vol. 301, p. 126881, 2019.

[7] H. Cho, X. Zhi, B. Wang, C. H. Ahn, and J. S. Go, "Development of a capacitive ice sensor to measure ice growth in a real time," in *2015 Transducers - 2015 18th International Conference on Solid-State Sensors, Actuators and Microsystems (TRANSDUCERS)*, 2015.

[8] "Piezoelectric sensor."

[9] A. Wajid, "On the accuracy of the quartz-crystal microbalance (qcm) in thin-film depositions," *Sensors and Actuators A: Physical*, vol. 63, no. 1, pp. 41–46, 1997.

[10] H. Law, P. Rossiter, G. Simon, and L. Koss, "Characterization of mechanical vibration damping by piezoelectric materials," *Journal of Sound and Vibration*, vol. 197, no. 4, pp. 489–513, 1996.

[11] "Vector network analyzer," accessed: 2023-10-23. [Online]. Available: https://en.wikipedia.org/wiki/Network_analyzer_(electrical)

[12] V. Upadhye and S. Agashe, "Effect of temperature and pressure variations on the resonant frequency of piezoelectric material," *Measurement and Control*, vol. 49, no. 9, pp. 286–292, 2016.

[13] C. M. Robinson and A. Jacobi, "A study of frost formation on a plain fin," *Air Conditioning and Refrigeration Center TR-188*, 2001.

[14] "Ad633 analog mixer," accessed: 2023-10-21. [Online]. Available: https://www.analog.com/media/en/technical-documentation/data-sheets/AD633-EP.pdf

[15] "The basics of mixers," accessed: 2023-10-21. [Online]. Available: https://www.digikey.com/en/articles/the-basics-of-mixers

[16] "Introduction to mixers," accessed: 2023-10-21. [Online]. Available: https://michaelgellis.tripod.com/mixersin.html

[17] J.-Y. Ryu, T.-C. Huynh, and J.-T. Kim, "Tension force estimation in axially loaded members using wearable piezoelectric interface technique," *Sensors*, vol. 19, no. 1, p. 47, 2018.

[18] "Piezoelectric sensor, cpt-2065-l100," accessed: 2023-10-21. [Online]. Available: https://www.mouser.com/datasheet/2/670/cpt_2065_l100-1777538.pdf

[19] "Sqp500jb-5r1," accessed: 2023-10-25. [Online]. Available: https://www.digikey.com/en/products/detail/yageo/SQP500JB-5R1/18648

[20] "B57891m0103k000," accessed: 2023-10-25. [Online]. Available: https://www.digikey.com/en/products/detail/epcos-tdk-electronics/B57891M0103K000/3500546

[21] J. M. Maldonado, A. de Gracia, G. Zsembinszki, P. Moreno, X. Albets, M. Á. González, and L. F. Cabeza, "Frost detection method on evaporator in vapour compression systems," *International Journal of Refrigeration*, vol. 110, pp. 75–82, 2020.

[22] S. Cao, L. Cui, and H. Liu, "Deep cost-sensitive learning for wheat frost detection," in *2022 3rd International Conference on Big Data, Artificial Intelligence and Internet of Things Engineering (ICBAIE)*. IEEE, 2022.

[23] D. P. Livingston, T. D. Tuong, J. P. Murphy, L. V. Gusta, I. Willick, and M. E. Wisniewski, "High-definition infrared thermography of ice nucleation and propagation in wheat under natural frost conditions and controlled freezing," *Planta*, vol. 247, pp. 791–806, 2018.

[24] Y.-H. Tai, A. S. A. Kamal, Y.-J. Park, P.-C. Tsai, Y.-L. Ho, P.-K. Wei, H. Daiguji, and J.-J. Delaunay, "Real-time monitoring of frost/defrost processes using a tapered optical fiber," *IEEE Sensors Journal*, vol. 21, no. 5, pp. 6188–6194, 2020.

[25] R. Kozak, B. D. Wiltshire, M. A. R. Khandoker, K. Golovin, and M. H. Zarifi, "Modified microwave sensor with a patterned ground heater for detection and prevention of ice accumulation," *ACS Applied Materials & Interfaces*, vol. 12, no. 49, pp. 55 483–55 492, 2020.

[26] R. Kozak, K. Khorsand, T. Zarifi, K. Golovin, and M. H. Zarifi, "Patch antenna sensor for wireless ice and frost detection," *Scientific Reports*, vol. 11, no. 1, p. 13707, 2021.